PHYSICAL REVIEW C **107**, 034318 (2023)

Excited states of zero seniority based on a pair condensate

Th. Popa and N. Sandulescu[*]
National Institute of Physics and Nuclear Engineering, 76900 Bucharest, Romania

M. Sambataro
Istituto Nazionale di Fisica Nucleare - Sezione di Catania, Via S. Sofia 64, I-95123 Catania, Italy

(Received 19 December 2022; accepted 2 March 2023; published 29 March 2023)

We study the excited states of zero seniority for various like-particle systems interacting by pairing forces and by general two-body interactions. We consider two types of excitations, generated from a ground state described by a pair condensate. One type is obtained by breaking a pair from the ground-state condensate and replacing it by "excited" collective pairs built on time-reversed single-particle orbits. The second type of zero-seniority excited states is described by a condensate of identical excited pairs. The structure of these excited states is analyzed for the picket fence model and for the valence neutrons of ^{108}Sn. For a state-depending pairing interaction, the first type of excited states agree well with the $J = 0$ states which are known in ^{108}Sn. At the same time, these states can be also associated unambiguously with those exact states which are the closest in energy to the experimental levels. The states corresponding to the excited pair condensate (EPC) appear at low energies, around the energy of the second-excited state of the first type, and they do not have a simple correspondence with exact eigenstates. However, at a much higher excitation energy there is an exact state which is similar in structure to an EPC state. It is shown that this EPC state has the features of a giant pairing vibration.

DOI: 10.1103/PhysRevC.107.034318

I. INTRODUCTION

As pointed out many years ago [1], basic nuclear properties can be simply explained in the framework of the BCS approach [2]. Presently, BCS-like approximations are employed to treat the pairing correlations in almost all mean-field calculations based on realistic energy density functionals (EDFs). The main drawback of these calculations is the fact that they break particle-number conservation. Restoring the right number of particles in the EDF calculations is not a trivial task [3]. The simplest alternative, which can be applied to any Hamiltonian in which the mean field and the pairing are decoupled, is to use from the beginning not the BCS but the particle-number projected-BCS (PBCS) approach [4–6]. Recall that, in the PBCS approach, the ground state is approximated by a pair condensate in which the number of pairs is fixed by the actual number of particles involved in the pairing calculations. The accuracy of BCS and PBCS approximations in describing ground-state properties of like-particle systems interacting by pairing forces has been analyzed in several studies. The main conclusions are the following: (a) BCS underestimates significantly the pairing correlations energies for finite systems, even in the limit of strong coupling [7]; (b) PBCS provides much better results [8], especially when applied in model spaces of the order of one major shell [9].

The BCS approach provides a simple scheme for understanding not only the ground-state properties of nuclei but also the pattern of their excitation spectra. In BCS the excited states are associated with quasiparticles generated by breaking particles from the BCS condensate and distributing them in single-particles states which are not participating to the pairing correlations. This is a rather crude approximation because it does not take into account the interaction between the quasiparticles and also because these excited states do not have a well-defined particle number. In addition, as pointed out already many years ago [7], in the BCS approximation one cannot unambiguously define the excited states of zero seniority. A better alternative is to start with the PBCS ansatz for the ground state and to construct excited states by breaking pairs from the PBCS condensate and replacing them by "excited" collective pairs (e.g., see Refs. [6,10–12] and the references quoted therein). In this study we shall focus on a particular type of these PBCS-based excited states, namely, the states of zero seniority. Apart from one-broken-pair states we also study another type of excited states of zero seniority. These excited states have the structure of a pair condensate built by identical excited pairs. The two types of zero-seniority excited states will be analyzed for various systems and their accuracy will be probed with Hamiltonians which can be solved exactly.

II. FORMALISM

In the present study we consider systems formed by an even number of spin-1/2 fermions, e.g., neutrons or protons, distributed on Ω single-particle states $|i\rangle$ of energies ϵ_i and interacting by a two-body force. For a force of pairing type

---

[*] Corresponding author: sandulescu@theory.nipne.ro

these systems are described by the Hamiltonian

$$H = \sum_{i}^{\Omega} \epsilon_i (a_i^\dagger a_i + a_{\bar{i}}^\dagger a_{\bar{i}}) + \frac{1}{4} \sum_{i,j=1}^{\Omega} v_{ij} a_i^\dagger a_{\bar{i}}^\dagger a_{\bar{j}} a_j. \qquad (1)$$

In the equation above, $\bar{i}$ denotes the time-reversed state $|\bar{i}\rangle = \hat{T}|i\rangle$ and $v_{ij} \equiv \langle i\bar{i}|\hat{V}|j\bar{j} - \bar{j}j\rangle$.

Usually, the ground and excited states of Hamiltonian (1) are approximated by employing BCS-based models. Here we focus on zero-seniority excited states which can be generated starting from the PBCS condensate. These states, introduced in Sec. II A, will be compared with the exact solutions of the Hamiltonian (1). For the state-independent pairing forces, i.e., $g = v_{ij}$, we use the exact analytical solutions found by Richardson many years ago [7]. The Richardson solutions, and their relations to the PBCS-based states, are presented shortly in the Sec. II B.

A. Zero-seniority states based on the projected-BCS condensate

In the BCS approximation, the ground state of Hamiltonian (1) is expressed as a coherent superposition of Cooper pairs, i.e.,

$$|BCS\rangle \propto e^{\Gamma^\dagger}|-\rangle \equiv \sum_n \frac{(\Gamma^\dagger)^n}{n!}|-\rangle, \qquad (2)$$

where the Cooper pairs are defined by

$$\Gamma^\dagger = \sum_i x_i a_i^\dagger a_{\bar{i}}^\dagger. \qquad (3)$$

The mixing amplitudes of the pair operator are usually written as $x_i = v_i/u_i$, where the parameters v_i and u_i are determined by solving the well-known BCS equations.

The particle number projected-BCS (PBCS) approximation is obtained by restricting the expansion in Eq. (2) to the term having the required number of pairs N. Thus, in PBCS the ansatz for the ground state is the pair condensate

$$|PBCS\rangle = (\Gamma^\dagger)^N|-\rangle. \qquad (4)$$

In the majority of applications the pairing is supposed to act only in a finite region around the Fermi level. In this case, N denotes only the particles involved in the pairing correlations, while the other particles of the system are included in the "vacuum" state $|-\rangle$.

The mixing amplitudes x_i of the pair operator (3) are determined variationally by minimizing the average of the Hamiltonian in the PBCS state (4) and imposing the normalization condition $\langle PBCS|PBCS\rangle = 1$. The corresponding PBCS equations satisfied by the parameters x_i can be found by employing the residual integrals technique [8]. Alternatively, if the number of pairs is not too large, the amplitudes x_i can be obtained by using the recurrence relations method [13]. These relations are given in the Appendix.

In the framework of PBCS approach the excited states are usually obtained by breaking pairs from the PBCS condensate and constructing new collective "excited" pairs which are attached to the remaining PBCS condensate [6,10–12]. In the present study we are interested in those excited states in which the excited collective pairs are built from pairs of fermions distributed in time reversed orbits. For the case of one-broken-pair approximation these excited states have the expression

$$|N; 1_k\rangle = \tilde{\Gamma}_k^\dagger (\bar{\Gamma}^\dagger)^{N-1}|0\rangle, \qquad (5)$$

where

$$\bar{\Gamma}^\dagger = \sum_i y_i a_i^\dagger a_{\bar{i}}^\dagger \qquad (6)$$

and

$$\tilde{\Gamma}_k^\dagger = \sum_i z_i^{(k)} a_i^\dagger a_{\bar{i}}^\dagger. \qquad (7)$$

The mixing amplitudes y_i and $z_i^{(k)}$ are determined variationally by minimizing the average of the Hamiltonian on the state (5) under the constraints $\langle N; 1_k|N; 1_{k'}\rangle = \delta_{k,k'}$ and $\langle N : 1_k|PBCS\rangle = 0$. It can be shown that these conditions are satisfied if the amplitudes $y_i^{(k)}$ and $z_i^{(k)}$ are satisfying the recurrence relations given in the Appendix.

In the same manner one can construct excited states with more broken pairs. Of special interest for this study are the excited states in which all the pairs are broken and replaced by a unique excited collective pair. These excited pair condensate (EPC) states have the expression

$$|EPC(k)\rangle = (\hat{\Gamma}_k^\dagger)^N|0\rangle, \qquad (8)$$

where $\hat{\Gamma}_k^\dagger = \sum_i w_i^{(k)} a_i^\dagger a_{\bar{i}}^\dagger$. The mixing amplitudes $w_i^{(k)}$ are determined variationally from the minimization of the average of the Hamiltonian on the state (8) under the constraints $\langle EPC(k)|EPC(k')\rangle = \delta_{k,k'}$ and $\langle EPC(k)|PBCS\rangle = 0$. The calculation scheme for the EPC states is similar to the one employed for the ground PBCS state.

As it can be noticed, in all the states introduced above the collective pairs are built as a superposition of two particles configurations $a_i^+ a_{\bar{i}}^+$. Due to this reason, these states are referred to as zero-seniority states. If the single-particle states are spherically symmetric, both the ground state and the excited states of the system defined by Eqs. (4), (5), and (8) have the angular momentum $J = 0$.

B. Zero-seniority states and the Richardson solution of state-independent pairing

As shown in Ref. [7], for a state-independent pairing interaction, the pairing Hamiltonian (1) can be solved analytically. For an even number of particles, the exact solution for the ground state has the expression [7]

$$|\Psi\rangle = \prod_{\nu}^{N} B_\nu^\dagger |0\rangle, \qquad (9)$$

where the pair operators $B_\nu^\dagger$ are defined by

$$B_\nu^\dagger = \sum_i \frac{1}{2\varepsilon_i - E_\nu} a_i^\dagger a_{\bar{i}}^\dagger. \qquad (10)$$

They depend on the parameters E_ν which satisfy the set of nonlinear equations

$$\frac{1}{g}-\sum_{j}\frac{1}{2\varepsilon_j-E_\nu}+\sum_{\mu\neq\nu}\frac{2}{E_\mu-E_\nu}=0. \tag{11}$$

The sum of the parameters E_ν gives the total energy of the system, i.e.,

$$E=\sum_{\nu}E_\nu. \tag{12}$$

In the limit $g=0$, the pair energies E_ν associated with the ground state coincide with twice the lowest single-particle energies, i.e., $E_\nu=2\varepsilon_\nu$, $(\nu=1,2,\dots,N)$, where N is the number of pairs. At specific finite values of the interaction strength, the pair energies turn two by two from real to complex-conjugate quantities.

There are two kinds of excited states which can be constructed starting from the ground state (9). One kind is obtained by breaking pairs and distributing the corresponding particles on different single-particle states, which will not participate in the pairing correlations. These excitations are analogous to BCS states of nonzero seniority. The second kind of excited states, corresponding to zero-seniority states, are obtained by keeping the number of collective pairs unchanged and modifying the initial conditions for the energies E_ν in the limit $g=0$. For example, the lowest excited state corresponds, in the limit $g=0$, to $E_\nu=2\epsilon_\nu$ for $\nu=1,2,\dots,N-1$ and $E_N=2\epsilon_{N+1}$. In Ref. [7] this excited state is labeled $(-1)^2(+1)^2$, indicating that this state is obtained, in the limit $g=0$ by promoting a pair from the last occupied level to the next unoccupied level. By this procedure one can generate excited states which have, formally, the same structure as the ground state (9), but expressed in terms of new "excited" B_ν pairs. The latter are defined by new parameters E_ν which are determined by solving the Richardson equations (11) with the new initial conditions at $g=0$.

As it can be seen, the exact and the PBCS-based states are quite different from each other. Contrasting them allows us to evince the limits of the PBCS approximations. For the PBCS-based states it is assumed that all the pairs B_ν^+ of the exact solution, except of an "excited" pair in the case of the states (5), can be represented by a unique collective pair Γ^+, which is supposed to average out the effect of the distinct pairs B_ν^+. This is a reasonable approximation for those pairs B_ν^+ which have similar structures. These are the pairs with the parameters E_ν not too far from the Fermi level and not too close to a single-particle energy. Consequently, the PBCS-based approximations are expected to work well if they are applied in a finite region around the Fermi level and for a rather strong pairing strength, typically greater than the critical BCS value.

Another difference between the exact and the PBCS-based solutions is in the number of parameters which defines them. In the case of the exact solution the number of parameters, E_ν, is equal to the number of pairs. On the other hand, for the PBCS-based states (4) and (8), the number of parameters is equal to the number of single-particle orbits included in the model space and twice this number for the states (5). Therefore, the accuracy of the PBCS-based approximations is expected to be better for large model spaces.

A specific feature of the exact solution, which is absent in the PBCS-based approximations, is the correlations between the B_ν^+ pairs. These correlations appear when some of the parameters E_ν become complex, which happens beyond a critical value of the pairing strength. In this case, the two pairs B_ν^+ corresponding to the complex-conjugate parameters (E_ν, E_ν^*) are entangled. More precisely, they form correlated four-body structures [14]. How important are these four-body structures in nuclei is still an open issue.

III. ACCURACY OF EXCITED STATES OF PROJECTED-BCS TYPE

To probe how well the approximations (5) and (8) work for the excited states, we consider first the case of a state-independent pairing Hamiltonian, which can be solved exactly by using the Richardson method. Then we shall analyze the PBCS-based states for a state-dependent pairing interaction and a general two-body force of shell-model type.

A. Excited states of zero seniority for a state-independent pairing force

We start by investigating the excited states for the systems formed by an even number of particles distributed in a set of equidistant and doubly degenerate levels. More precisely, we consider Ω levels of energies $\epsilon_i=1,2,\dots,\Omega$, and a number of particles corresponding to half filling, i.e., $2N=\Omega$, where N is the number of pairs. These systems, with $N=4$–16, have been considered by Richardson in order to analyze the performance of the BCS approximation relative to the exact solution [7]. Similar systems, with $N=4$–40, have been used later to analyze the accuracy of the PBCS approximation for the ground state [9].

Here we take as an example a system with $N=4$ and $\Omega=8$. As for the pairing strength, we use the same range employed by Richardson, i.e., $g=0.7$–1.1. For this system there are eight zero-seniority states of the form (5). The energies of these states are shown in Fig. 1. For the lowest state the collective pairs (6) and (7) have a similar structure and both of them are similar to the ground-state pair Γ^+ of the PBCS condensate (4). Therefore, the state (5) with the lowest energy shown in Fig. 1 corresponds to the PBCS ground state.

The first-excited state (5) is calculated by variationally determining both the pair $\bar{\Gamma}^+$ of the broken condensate and the excited pair. A simpler approximation, which we apply for the higher excited states (5), is to keep for $\bar{\Gamma}^+$ the same structure as for the ground state.

For comparison, Fig. 1 also shows the exact energies for the lowest eight states of zero seniority. The first energy corresponds to the ground state while the second corresponds to the Richardson solution denoted by $(-1)^2(+1)^2$, i.e., a state which is obtained, in the limit $g=0$, by promoting a pair from the last occupied level to the first unoccupied level. The next energies correspond to doubly degenerate solutions. For example, the third energy corresponds to the third and the fourth degenerate states. In the limit $g=0$ these states correspond to

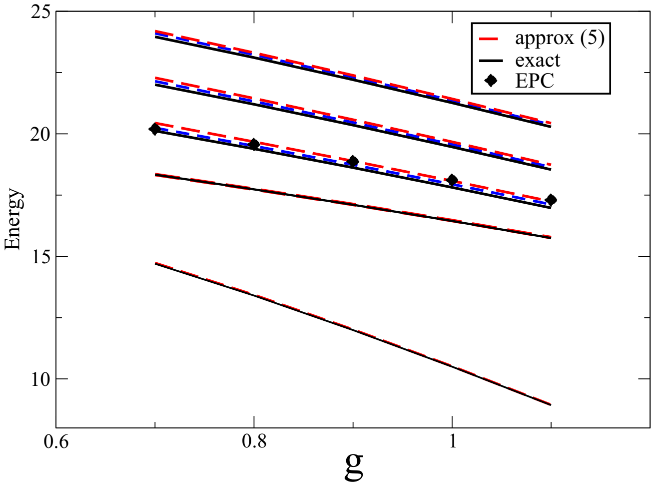

FIG. 1. The energies of the states (4) and (5) compared with the exact results as a function of pairing strength. By full diamonds we show the energies of the excited pair condensate (8). The results correspond to four pairs distributed in eight equidistant and doubly degenerate states. The energies and the pairing strength are given in units of single-particle level spacings.

the configurations $(-1)^2(+2)^2$ and $(-2)^2(+1)^2$, which have the same energies.

From Fig. 1 one can notice that the ground-state energy predicted by PBCS is very accurate. Indeed, the maximum deviation from the exact value, corresponding to $g = 1.1$, is about 0.26%. The energies of excited states (5) follow rather closely the exact energies. In particular one can see that to the exact doubly degenerate states correspond to two nondegenerate states (5) with energies close to the exact value.

The energy of the lowest excited pair condensate (EPC) is shown in Fig. 1 by full diamonds. It can be seen that the EPC energy follows closely the exact energy of the third and the fourth degenerate states. The energy of the EPC state is unexpectedly low, taking into account the fact that this state is obtained by breaking all the pairs from the ground-state condensate.

An indication of how close the wave functions (4), (5), and (8) are to the exact states is obtained from the comparison between the predicted occupation probabilities of the single-particle orbits. This comparison is done here for the strength $g = 0.7$. The occupation probabilities v_i^2 corresponding the ground state (4) and the first-excited state (5) are shown in Figs. 2(a) and 2(b). As it can be seen, the v_i^2 for these states follow the exact results rather closely, especially for the ground state (4).

A comparison with the exact wave functions corresponding to the doubly degenerate states is not straightforward. This is because any combination of the two degenerate solutions is also exact eigenfunction of the Hamiltonian. Due to this reason the occupation probabilities $v_i^2(1)$ and $v_i^2(2)$ associated with the two degenerate states are not well-defined because they depend on the chosen representation for these states. What does not depend on the representation is the sum $v_i^2(12) = v_i^2(1) + v_i^2(2)$. In Figs. 2(c)–2(e) one can see the comparison between $v_i^2(12)$ and v_i^2 associated with the two states (5) which are closest in energy to the exact degenerate states. It can be seen that v_i^2 and $v_i^2(12)$ are rather similar.

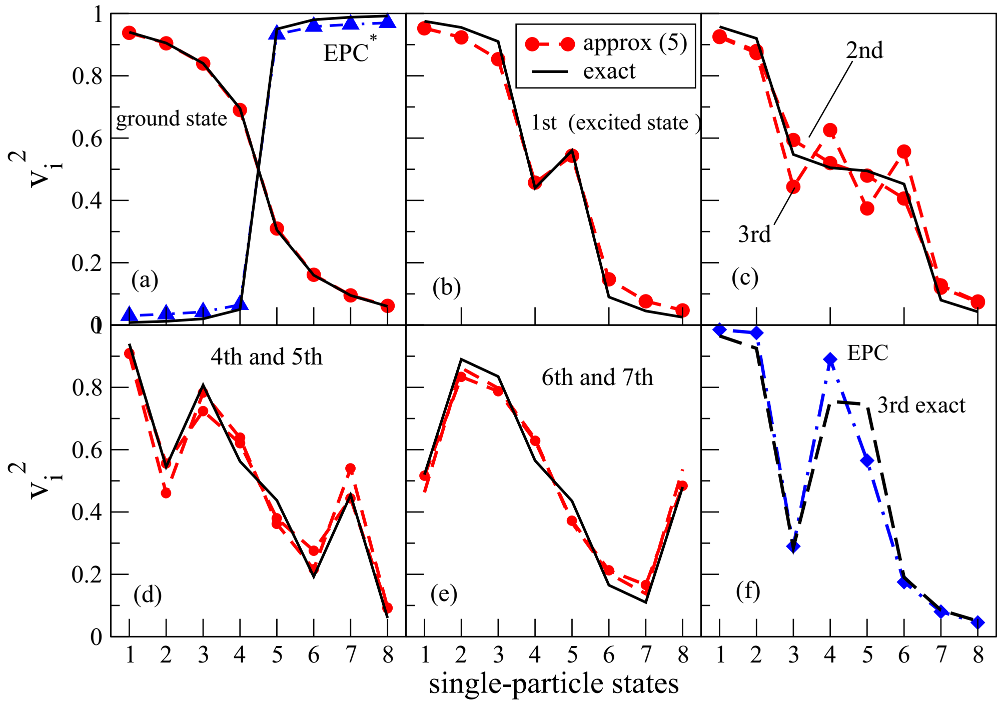

FIG. 2. Occupation probabilities of single-particle states for the states (4), (5), and (8) and the exact states which are closest in energy. For the exact degenerate states we show the sum of the occupation probabilities. For the states EPC* and EPC shown in panels (a) and (f), see the text. The results are for the pairing strength $g = 0.7$.

The occupation probabilities v_i^2 corresponding to the EPC state are shown in Fig. 2(f). In the limit $g = 0$ the EPC state corresponds to the configuration $(-1)^2(+2)^2$. Since, in the limit $g = 0$, this is also the configuration of the third exact state, we expect that the latter to be closer to the EPC state. To check that, we have done another calculation in which we have removed the degeneracy of the exact states by adding a very small perturbation. The v_i^2 corresponding to the third new state are shown in Fig. 2(f) by dashed-dotted line. One can notice that the v_i^2 corresponding to the exact state and to the EPC state are rather different for the fourth and the fifth single-particle orbits. This indicates that the EPC state shown in Fig. 1 has a structure which is distinct from that of the nearby exact states.

An interesting question is whether there is an exact eigenstate of the Hamiltonian which is similar in structure to a EPC state. To answer this question, for each exact eigenstate $|\Psi\rangle$ of zero seniority we determined the EPC state which maximizes the overlap $\langle EPC|\Psi\rangle$ and which is orthogonal to the ground-state pair condensate. We found that the eigenstate $|\Psi\rangle$ with the highest energy, equal to -49.935, is the one that resembles the most a EPC state. The overlap of this eigenstate with the corresponding EPC state, called below the EPC* state, is equal to 0.986. The energy of the EPC* state is equal to -49.596, a value rather close to the exact energy of the $|\Psi\rangle$ state. The occupation probabilities v_i^2 of the single-particle orbits for the EPC* state are shown in Fig. 2(a). As can be seen, they follow closely the exact values. By contrast to the EPC state shown in Fig. 2(f), the occupation probabilities for the EPC* state have a smooth dependence on single-particle energies, as in the case of the ground-state condensate. As seen from Fig. 2(a), the EPC* state looks as the reverse of the ground-state condensate, in the sense that in the two states the role of the lower and higher energy orbitals is interchanged.

B. Excited states of zero seniority for a state-dependent pairing force

To benchmark the accuracy of the states (4), (5), and (8) in the case of state-dependent pairing forces, we consider a pairing interaction derived from G-matrix calculations [15]. Its matrix elements and the energies of the single-particle states are given in Ref. [16]. With this interaction we have calculated the zero seniority states for ^{108}Sn, taking ^{100}Sn as core. As in the previous section, the first-excited state (5) is calculated by variationally determining both the excited pair and the pair $\bar{\Gamma}^+$ which defined the broken pair condensate. For the other excited states we determine variationally only the excited pair while for the pair $\bar{\Gamma}^+$ we take the same structure as for the ground-state condensate.

The predictions of the states (4), (5), and (8) for the energies are shown in Fig. 3. In the same figure we show the energies of the exact states with $J = 0$ obtained by diagonalization. The exact energies which correspond to the states (4), (5) are indicated by dashed lines. This correspondence is supported by the very good agreement between the occupation probabilities of the orbits, shown in Fig. 4.

Figure 3 also includes the experimentally known levels which, most probably, have the spin $J = 0$. One can notice that the energies of these levels are reasonably described by the states (5). The largest discrepancy is for the first-excited state, which is predicted at lower energy. In the energy region of the experimental levels there are six exact $J = 0$ states. It can be seen that the exact states which are the closest to experimental levels are those which correspond to the three lowest states (5). Consequently, it appears that the lowest three known $J = 0$ states in ^{108}Sn have a simple physical interpretation: they have a structure of one-broken-pair type.

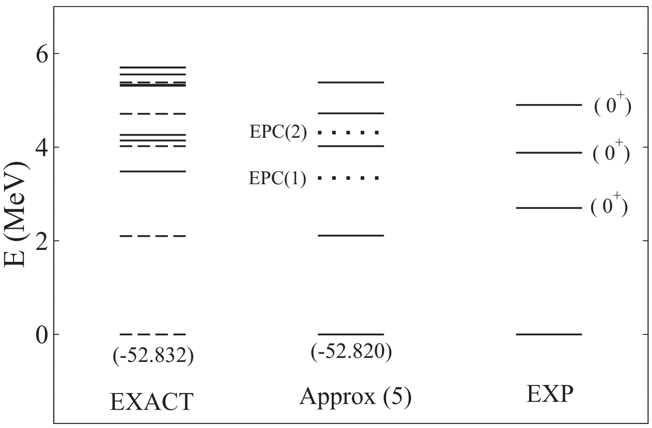

FIG. 3. Energies corresponding to the states (4), (5), and (8) compared with the exact spectrum and experimental energies [17]. The exact energies which correspond to the states (4), (5) are indicated by dashed line. EPC are the energies of the excited pair condensate. The numbers within round brackets are the ground-state energies, in MeV. All calculated levels have $J = 0$. The results are for the neutrons in the valence shell of ^{108}Sn interacting through a state-dependent pairing interaction.

In Fig. 3 are shown the energies of two EPC states (8). They correspond to the first two minima obtained variationally with the state (8). The occupation probabilities of the single-particle states corresponding to the two EPC states are shown in Fig. 4(f). The lowest EPC state is practically built on the first two single-particle orbitals, $g_{7/2}$ and $d_{5/2}$. On the other hand, the second EPC state is spread out on all the orbits. In the limit of small pairing strength the two EPC states correspond to three pairs promoted from the orbit $g_{7/2}$ to the orbit $d_{5/2}$ and, respectively, to one pair promoted from $g_{7/2}$ to $3s_{1/2}$. In the Richardson notations these configurations are $(-1)^6(+1)^6$ and $(-1)^2(+2)^2$. In the energy region of the EPC states there are few exact states. In Fig. 4(f) we show the comparison with the third exact excited state, which has the closest similarity to the EPC(2) state. It can be noticed that this exact state has a significantly lower occupation probability for the orbit $3s_{1/2}$. Summarizing, the EPC states (8) have a peculiar structure, different from the eigenstates of the pairing Hamiltonian and different also from the experimentally known $J = 0$ states.

As in the case of the picket fence model, we have searched whether there is an exact eigenstate of the state-depending pairing Hamiltonian which is similar in structure to a EPC state. To find this state we have used the procedure we explained at the end of the previous section. The search was done for the 49 exact seniority-zero states obtained by

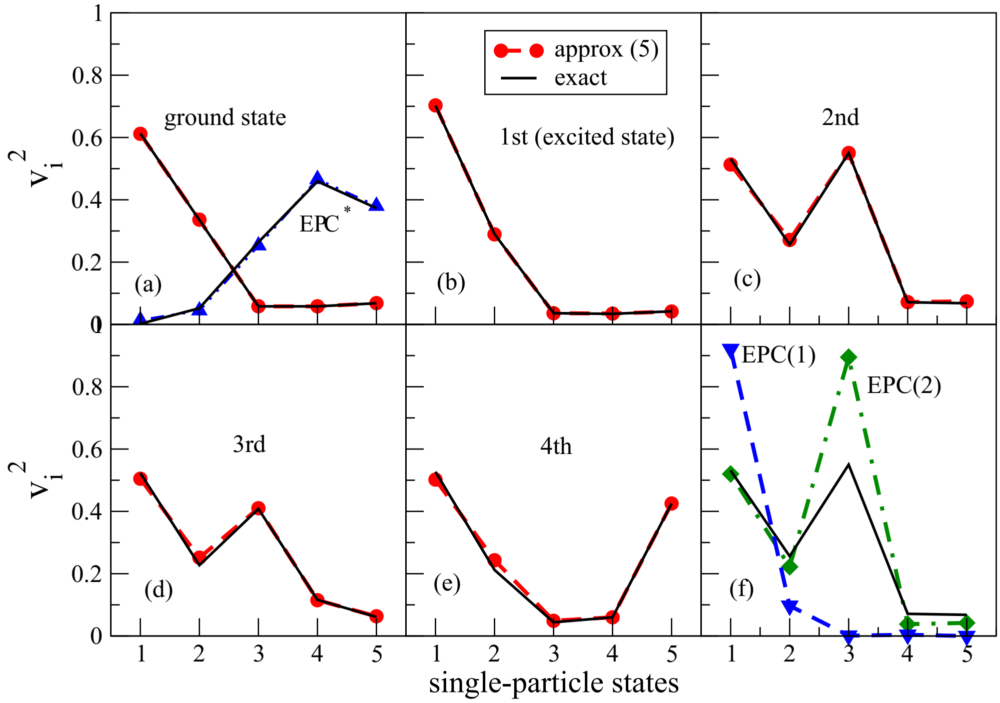

FIG. 4. Occupation probabilities of single-particle (s.p.) orbits corresponding to the states (4), (5), and (8) compared with the exact states which have the closest similarity with the former. For the states EPC* and EPC(1,2) shown in panels (a) and (f), see the text. The five s.p. states on the x axis are, from the left to the right, $1g_{7/2}$, $2d_{5/2}$, $3s_{1/2}$, $1h_{11/2}$, and $2d_{3/2}$. The results are for the neutrons in the valence shell of ^{108}Sn interacting through a state-dependent pairing interaction.

diagonalizing the Hamiltonian in the space of pairs. We have found that the 46th state, of energy -31.854, resembles the most an EPC state. This eigenstate has the largest overlap with an EPC state, equal to 0.995. The EPC state, which we shall denote by EPC*, as in the previous section, has an energy equal to -31.905, which is very close to the energy of the corresponding exact state. The occupation probabilities of the single-particle orbits associated with the EPC* state are shown in Fig. 4(a). As can be seen, they can be hardly distinguished from the occupation probabilities of the corresponding exact state. From Fig. 4(a) one can notice that the EPC* state is mainly built on the high-energy orbits $1h_{11/2}$ and $2d_{3/2}$. This is the reversed situation compared with the ground-state condensate, in which the low-energy orbits $1g_{7/2}$ and $2d_{5/2}$ have the highest occupation probabilities.

In the context of tin isotopes, the EPC* state discussed above has common features with the so-called giant pairing vibration (GPV). For a recent overview of the theoretical and experimental work done on GPV, see Ref. [18]. Here we recall that the GPV is usually defined as a collective excited state composed of a coherent superposition of particle-particle configurations, analogous to the ground state. However, contrary to the ground state, the GPV state is expected to be formed by a particle-particle configuration built on the next major shell rather than the valence shell. This is the standard scenario for the formation of the GPV state, which was initially considered for the case of lead isotopes [19,20]. The light tin isotopes, in particular the isotope ^{108}Sn considered in this paper, offer an interesting alternative to the standard scenario mentioned above. As it is known, in tin isotopes the neutron number $N = 64$ is a quasimagic number. This is due to the fact that the lowest two orbits $1g_{7/2}$ and $2d_{5/2}$ are rather well separated in energy from the last two orbits $1h_{11/2}$ and $2d_{3/2}$. In between these orbits there is the state $3s_{1/2}$, but, since its degeneracy is small, this state does not affect much the quasimagic character of $N = 64$. Consequently, since in ^{108}Sn the two first orbits play the role of the valence shell while the last two orbits act as the next major shell, the EPC* state discussed above has the characteristic of a GPV state built on the orbits $1h_{11/2}$ and $2d_{3/2}$.

C. Excited states of zero seniority for a general shell-model-type interaction

To analyze the zero-seniority states for the case of a general two-body force we consider as an example a shell-model interaction [21] which was fit in order to get a reasonable description of the low-lying states of tin isotopes [22]. The one-broken-pair approximation was applied for tin isotopes and realistic interactions in various studies [10–12,23], but in none of them the accuracy of this approximation was analyzed for the excited states of zero seniority. Here we examine the states of zero seniority for the tin isotope ^{108}Sn and the predictions of the approximations (4), (5), and (8) will be compared with the exact solutions provided by exact diagonalization.

All excited states (5) are calculated by replacing the pair $\bar{\Gamma}^+$, which defines the broken condensate, by the pair of the ground-state condensate (4). The energies of the states (4), (5), and (8) are shown in Fig. 5. In Fig. 5 we also show the exact shell-model (SM) energies, calculated with the code BIGSTICK

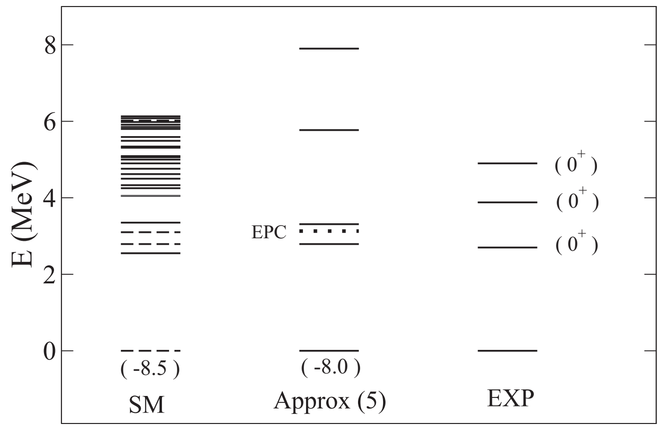

FIG. 5. The same as in Fig. 3 but for a general two-body force of shell-model type.

[24]. As expected, for the case of the general interaction the correspondence between the states (5) and the exact states is not so straightforward as for the pairing interactions. First of all, from the occupation probabilities shown in Fig. 6 we observe that the SM ground state can be well approximated by a pair condensate. There is also a very good agreement between the first-excited state (5) and the second SM excited state. The second state (5) corresponds to the fourth SM excited state, but the agreement between the occupation probabilities is not as good as for the first-excited state. In the energy region of the third and the fourth excited states (5) there are many SM states, which make the comparison difficult. In Fig. 6 we have shown the comparison with the SM states which we found to have the closest resemblance in occupation probabilities. As it can be seen, for these states the differences are significant.

From Fig. 5 one can notice that the PBCS approximation provides a binding energy which is very close to the exact result. There is also a very good agreement between the energies of the second excited SM, the first one-broken-pair state and the first experimental $J = 0$ level. Surprisingly, the agreement between the other experimental $J = 0$ states and the calculated states is less good for the general interaction than for the state-dependent pairing interaction.

From Fig. 5 one can observe that the energy of the lowest EPC state is between the first and the second-excited state (5). At $g = 0$ this state corresponds to a pair moved from $g_{7/2}$ to $3s_{1/2}$. The occupation probabilities corresponding to the EPC state are shown in Fig. 6(f). In the same figure are shown the occupation probabilities corresponding to the third SM state, which has the closest resemblance to the structure of the EPC state. As in the case of state-depending pairing interaction, the occupation probability for the state $3_{1/2}$ is much larger for the EPC state than for the exact state.

At high excitation energies the SM calculations with the general interaction predict a very large number of $J = 0$ states. As illustrated in Fig. 5, this happens already for energies around 6 MeV. For this reason, it is difficult to search for the SM level which has the closest resemblance with a EPC state, as we have done for the pairing forces.

IV. SUMMARY AND CONCLUSIONS

We have analyzed the properties of excited states of zero seniority generated from the ground-state pair condensate. One type of zero-seniority state is obtained by breaking a pair from the pairing condensate and replacing it with an "excited" pair. In addition, we have also considered a second type of

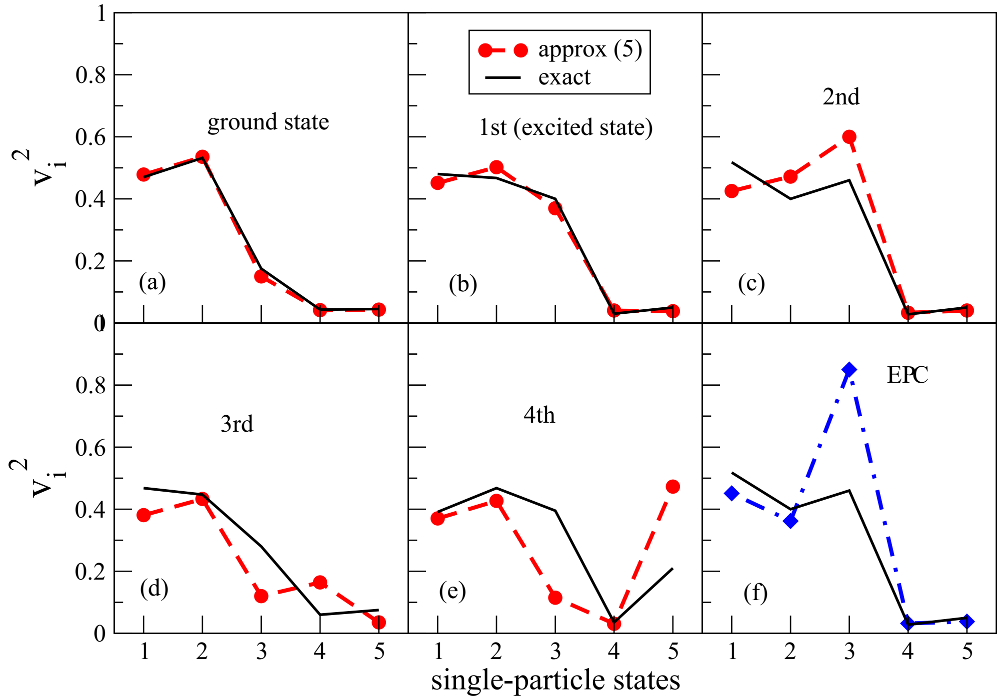

FIG. 6. The same as in Fig. 4 but for a general two-body force of shell-model type.

excited state which are obtained by breaking all the pairs from the ground-state condensate and replacing them with identical excited pairs. The first and the second type of zero-seniority states are referred to as one-broken-pair and, respectively, excited pair condensate (EPC) states. These states have been analyzed for the picket fence model and for the nucleus ^{108}Sn. For this nucleus we first performed a calculation with a state-dependent pairing interaction which is commonly used for tin isotopes. We found that the one-broken-pair states agree well with the known $J = 0$ states in ^{108}Sn. In the energy region of the one-broken-pair states there are many exact $J = 0$ states, more than the experimentally known levels. Among the exact states one can identify some states which are very similar in energy and structure to the one-broken-pair states. Based on these results, we concluded that the experimentally known $J = 0$ excited states in ^{108}Sn are of one-broken-pair type.

For a state-independent pairing force we have first analyzed the EPC states which minimize the average of the pairing Hamiltonian. We have identified two such EPC states, which appear at low energies, between the first and the third one-broken-pair states. In this energy region we did not find exact states similar in structure to the two EPC states. However, at a much higher excitation energy, of about 20 MeV, we have found an exact state which is similar in structure to an EPC state. This EPC state, denoted EPC*, is the reverse of the ground-state condensate in the sense that it is built on the highest energy orbitals instead of the lowest one. It is shown that the EPC* state has the features of a pairing vibration state.

We have also analyzed the zero-seniority states in ^{108}Sn for a general shell-model type interaction which was fit to describe the low-lying states in tin isotopes. Compared with the previous case, the agreement between the one-broken pair states and the experimentally known $J = 0$ states is better for the first level but less good for the other levels. In the region of the high-energy states there are many shell-model states with $J = 0$, which makes difficult the comparison with the experimental data and also to the one-broken-pair states. For the general interaction we found also a EPC state of relatively low excitation energy. Whether one could excite nuclei in such a particular low-energy state, described by a pair condensate, is an interesting question which deserves further studies.

ACKNOWLEDGMENTS

We thank Daniel Negrea for participating to the initial phase of this study. N.S. is grateful for the hospitality of Institute of Modern Physics, Cantabria University, Spain, where this paper was mainly designed and written. Th.P. acknowledges a Ph.D. fellowship from the University of Bucharest. This work is supported by a grant of the Romanian Ministry of Research and Innovation, CNCS - UEFISCDI, project number PCE 160/2021, within PNCDI III, and by PN 23210101/2023.

APPENDIX

In this Appendix we provide the recurrence relations necessary to calculate the average of the pairing Hamiltonian in the states (4) and (5) as well as the norm of these states. We consider the case of spherically symmetric single-particle levels and we label them by the standard quantum numbers $|n_i l_i j_i m_i\rangle \equiv |i m_i\rangle$. We express the Hamiltonian in terms of spherically symmetric quantities, i.e.,

$$H = \sum_i^{\Omega} \epsilon_i N_{j_i} + \sum_{ij=1}^{\Omega} V_{ij} P_i^\dagger P_j, \tag{A1}$$

where $V_{ij} = \sqrt{(2j_i+1)(2j_j+1)}\langle (ii)J = 0|V|(jj)J = 0\rangle$. The operators $P^\dagger$ represent a pair of angular momentum $J = 0$, i.e.,

$$P_i^\dagger = \frac{1}{\sqrt{2j_i+1}} \sum_{m_i=-j_i}^{j_i} (-1)^{j_i - m_i} a_{m_i}^\dagger a_{-m_i}^\dagger. \tag{A2}$$

In what follows the states (4) and (5) are denoted by

$$|n; 0\rangle = (\Gamma^\dagger)^n |0\rangle, \tag{A3}$$

$$|n; 1\rangle = \tilde{\Gamma}^\dagger (\bar{\Gamma}^\dagger)^{N-1} |0\rangle. \tag{A4}$$

Since the variational calculations involved only one state (5) at a time, in Eq. (16) we have removed the index k. With these notations the collective pair operators have the expressions

$$\overline{\Gamma}^\dagger = \sum_i x_i P_i^\dagger, \tag{A5}$$

$$\tilde{\Gamma}^\dagger = \sum_i y_i P_i^\dagger. \tag{A6}$$

Below we give the recurrence relations for the overlaps and for the operators which are involved in calculating the average of the pairing Hamiltonian. For all the recurrence relations we provide also the initial quantities required to evolve them.

1. Recurrence relations for the overlaps

$$\langle n, 0|n, 0\rangle = n \sum_i x_i^2 \langle n-1, 0|n-1, 0\rangle - 2n(n-1) \sum_i \frac{x_i^3}{2i+1} \langle n-2, 0|P_i|n-1, 0\rangle$$

$$\langle n-1, 1|n, 0\rangle = (n-1) \sum_i x_i^2 \langle n-2, 1|n-1, 0\rangle + \sum_i x_i y_i \langle n-1, 0|n-1, 0\rangle - 2(n-1)(n-2) \sum_i \frac{x_i^3}{2i+1}$$
$$\times \langle n-3, 1|P_i|n-1, 0\rangle - 4(n-1) \sum_i \frac{x_i^2 y_i}{2i+1} \langle n-2, 0|P_i|n-1, 0\rangle \langle n, 1|n, 1\rangle$$

$$
\begin{aligned}
&= n\sum_i x_i y_i \langle n-1,1|n,0\rangle + \sum_i y_i^2 \langle n,0|n,0\rangle \\
&\quad -2n(n-1)\sum_i \frac{x_i^2 y_i}{2i+1}\langle n-2,1|P_i|n,0\rangle - 4n\sum_i \frac{x_i y_i^2}{2i+1}\langle n-1,0|P_i|n,0\rangle .
\end{aligned}
$$

The initial quantities are

$$
\langle 1,0|1,0\rangle = \sum_i x_i^2, \quad \langle 1,0|0,1\rangle = \sum_i x_i y_i, \quad \langle 0,1|1,0\rangle = \sum_i x_i y_i, \quad \langle 0,1|0,1\rangle = \sum_i y_i^2 .
$$

2. Recurrence relations for the particle number operator N_i

$$
\begin{aligned}
&\langle n,0|N_i|n,0\rangle = 2nx_i\langle n-1,0|P_i|n,0\rangle, \quad \langle n-1,1|N_i|n,0\rangle = 2nx_i\langle n-1,0|P_i|n-1,1\rangle, \\
&\langle n,1|N_i|n,1\rangle = 2nx_i\langle n-1,1|P_i|n,1\rangle + 2y_i\langle n,0|P_i|n,1\rangle .
\end{aligned}
$$

The initial quantities are

$$
\langle 1,0|N_i|1,0\rangle = 2x_i^2, \quad \langle 1,0|N_i|0,1\rangle = 2x_i y_i, \quad \langle 0,1|N_i|1,0\rangle = 2x_i y_i, \quad \langle 0,1|N_i|0,1\rangle = 2y_i^2 .
$$

3. Recurrence relations for the pair operator P_i

$$
\begin{aligned}
\langle n-1,0|P_i|n,0\rangle &= nx_i\langle n-1,0|n-1,0\rangle - \frac{2n(n-1)}{2i+1}x_i^2\langle n-2,0|P_i|n-1,0\rangle, \\
\langle n-2,1|P_i|n,0\rangle &= nx_i\langle n-2,1|n-1,0\rangle - \frac{2n(n-1)}{2i+1}x_i^2\langle n-2,0|P_i|n-2,1\rangle, \\
\langle n-1,1|P_i|n,1\rangle &= nx_i\langle n-1,1|n-1,1\rangle + y_i\langle n-1,1|n,0\rangle \\
&\quad -\frac{2n(n-1)}{2i+1}x_i^2\langle n-2,1|P_i|n-1,1\rangle - \frac{4n}{2i+1}x_i y_i\langle n-1,0|P_i|n-1,1\rangle .
\end{aligned}
$$

The initial quantities are

$$
\langle -|P_i|1,0\rangle = x_i, \quad \langle -|P_i|0,1\rangle = y_i .
$$

4. Recurrence relations for the pairing interaction operator $P_i^\dagger P_j$

$$
\begin{aligned}
&\langle n,0|P_i^\dagger P_j|n,0\rangle \\
&\quad = n^2 x_i x_j\langle n-1,0|n-1,0\rangle - \frac{2n^2(n-1)}{2j+1}x_i x_j^2\langle n-2,0|P_j|n-1,0\rangle \\
&\quad -\frac{2n^2(n-1)}{2i+1}x_i^2 x_j\langle n-2,0|P_i|n-1,0\rangle + \frac{2n(n-1)}{2i+1}\frac{2n(n-1)}{2j+1}x_i^2 x_j^2\Bigg[\langle n-2,0|P_j^\dagger P_i|n-2,0\rangle \\
&\quad +\delta_{ij}\left(\langle n-2,0|n-2,0\rangle - \frac{2}{2i+1}\langle n-2,0|N_i|n-2,0\rangle\right)\Bigg], \\
&\langle n-1,1|P_i^\dagger P_j|n,0\rangle \\
&\quad = n(n-1)x_i x_j\langle n-2,1|n-1,0\rangle - \frac{2n(n-1)^2}{2j+1}x_i x_j^2\langle n-2,0|P_j|n-2,1\rangle \\
&\quad +nx_j y_i\langle n-1,0|n-1,0\rangle - \frac{2n(n-1)}{2j+1}x_j^2 y_i\langle n-2,0|P_j|n-1,0\rangle \\
&\quad -\frac{2n(n-1)(n-2)}{2i+1}x_i^2 x_j\langle n-3,1|P_i|n-1,0\rangle \\
&\quad +\frac{2(n-1)(n-2)}{2i+1}\frac{2n(n-1)}{2j+1}x_i^2 x_j^2\Bigg[\langle n-3,1|P_j^\dagger P_i|n-2,0\rangle
\end{aligned}
$$

$$
\begin{aligned}
&+\delta_{ij}\bigg(\langle n-3,1|n-2,0\rangle-\frac{2}{2i+1}\langle n-3,1|N_i|n-2,0\rangle\bigg)\bigg]-\frac{4n(n-1)}{2i+1}x_ix_jy_i\langle n-2,0|P_i|n-1,0\rangle\\
&+\frac{4(n-1)}{2i+1}\frac{2n(n-1)}{2j+1}x_ix_j^2y_i\bigg[\langle n-2,0|P_j^\dagger P_i|n-2,0\rangle\\
&+\delta_{ij}\bigg(\langle n-2,0|n-2,0\rangle-\frac{2}{2i+1}\langle n-2,0|N_i|n-2,0\rangle\bigg)\bigg],
\end{aligned}
$$

$$
\begin{aligned}
&\langle n,1|P_i^\dagger P_j|n,1\rangle\\
&\quad=n^2x_ix_j\langle n-1,1|n-1,1\rangle+nx_iy_j\langle n-1,1|n,0\rangle\\
&\quad-\frac{2n^2(n-1)}{2j+1}x_ix_j^2\langle n-2,1|P_j|n-1,1\rangle-\frac{4n^2}{2j+1}x_ix_jy_j\langle n-1,0|P_j|n-1,1\rangle\\
&\quad+nx_jy_i\langle n,0|n-1,1\rangle+y_iy_j\langle n,0|n,0\rangle-\frac{2n(n-1)}{2j+1}x_j^2y_i\langle n-2,1|P_j|n,0\rangle\\
&\quad-\frac{4n}{2j+1}x_jy_iy_j\langle n-1,0|P_j|n,0\rangle-\frac{2n^2(n-1)}{2i+1}x_i^2x_j\langle n-2,1|P_i|n-1,1\rangle\\
&\quad-\frac{2n(n-1)}{2i+1}x_i^2y_j\langle n-2,1|P_i|n,0\rangle+\frac{4n^2(n-1)^2}{(2j+1)^2}x_i^2x_j^2\bigg[\langle n-2,1|P_j^\dagger P_i|n-2,1\rangle\\
&\quad+\delta_{ij}\bigg(\langle n-2,1|n-2,1\rangle-\frac{2}{2i+1}\langle n-2,1|N_i|n-2,1\rangle\bigg)\bigg]\\
&\quad+\frac{8n^2(n-1)}{(2j+1)^2}x_i^2x_jy_j\bigg[\langle n-2,1|P_j^\dagger P_i|n-1,0\rangle+\delta_{ij}\bigg(\langle n-2,1|n-1,0\rangle-\frac{2}{2i+1}\langle n-2,1|N_i|n-1,0\rangle\bigg)\bigg]\\
&\quad-\frac{4n^2}{2i+1}x_ix_jy_i\langle n-1,0|P_i|n-1,1\rangle-\frac{4n}{2i+1}x_iy_iy_j\langle n-1,0|P_i|n,0\rangle+\frac{8n^2(n-1)}{(2j+1)^2}x_ix_j^2y_i\\
&\quad\times\bigg[\langle n-1,0|P_j^\dagger P_i|n-2,1\rangle+\delta_{ij}\bigg(\langle n-1,0|n-2,1\rangle-\frac{2}{2i+1}\langle n-1,0|N_i|n-2,1\rangle\bigg)\bigg]\\
&\quad+\frac{16n^2}{(2i+1)^2}x_ix_jy_iy_j\bigg[\langle n-1,0|P_j^\dagger P_i|n-1,0\rangle+\delta_{ij}\bigg(\langle n-1,0|n-1,0\rangle-\frac{2}{2i+1}\langle n-1,0|N_i|n-1,0\rangle\bigg)\bigg].
\end{aligned}
$$

The initial quantities are

$$
\langle 1,0|P_i^\dagger P_j|1,0\rangle=x_ix_j,\quad\langle 1,0|P_i^\dagger P_j|0,1\rangle=x_iy_j,\quad\langle 0,1|P_i^\dagger P_j|1,0\rangle=x_jy_i,\quad\langle 0,1|P_i^\dagger P_j|0,1\rangle=y_iy_j.
$$

[1] A. Bohr, B. Motelsson, and D. Pines, Phys. Rev. **110**, 936 (1958).

[2] J. Bardeen, L. N. Cooper, and J. R. Schrieffer, Phys. Rev. **108**, 1175 (1957).

[3] J. A. Sheikh, J. Dobaczewski, P. Ring, L. M. Robledo, and C. Yanouleas, J. Phys. G **48**, 123001 (2021).

[4] B. F. Bayman, Nucl. Phys. **15**, 33 (1960).

[5] M. Blatt, Prog. Theor. Phys. **24**, 851 (1960).

[6] I. Talmi, Nucl. Phys. A **172**, 1 (1971).

[7] W. Richardson, Phys. Rev. **141**, 949 (1966).

[8] K. Dietrich, H. J. Mang, and J. H. Pradal, Phys. Rev. **135**, B22 (1964).

[9] N. Sandulescu and G. F. Bertsch, Phys. Rev. C **78**, 064318 (2008).

[10] Y. K. Gambhir, A. Rimini, and T. Weber, Phys. Rev. C **3**, 1965 (1971).

[11] G. Bonsignori, M. Savoia, K. Allaart, A. van Egmond, and G. Te Velde, Nucl. Phys. A **432**, 389 (1985).

[12] K. Allaart, E. Boeker, G. Bonsignori, M. Savoia, and Y. K. Gambhir, Phys. Rep. **169**, 209 (1988).

[13] N. Sandulescu, B. Errea, and J. Dukelsky, Phys. Rev. C **80**, 044335 (2009).

[14] M. Sambataro and N. Sandulescu, J. Phys. G **40**, 055107 (2013).

[15] A. Holt, T. Engeland, M. Hjorth-Jensen, and E. Osnes, Nucl. Phys. A **634**, 41 (1998).
[16] V. Zelevinsky and A. Volya, Phys. At. Nucl. **66**, 1781 (2003).
[17] https://www.nndc.bnl.gov/
[18] M. Assié, C. H. Dasso, R. J. Liotta, A. Macchiavelli, and A. Vitturi, Eur. Phys. J. A **55**, 245 (2019).
[19] R. A. Broglia and D. R. Bes, Phys. Lett. B **69**, 129 (1977).
[20] M. W. Herzog, R. J. Liotta, and T. Vertse, Phys. Lett. B **165**, 35 (1985).
[21] http://www.nuclear.kth.se/cqi/sn100/files/MC-Oxbash.txt.
[22] Chong Qi (private communication).
[23] N. Sandulescu, J. Blomqvist, T. Engeland, M. Hjorth-Jensen, A. Holt, R. J. Liotta, and E. Osnes, Phys. Rev. C **55**, 2708 (1997).
[24] C. W. Johnson, W. E. Ormand, and P. G. Krastev, Comput. Phys. Commun. **184**, 2761 (2013).